PHYSICAL REVIEW B **84**, 245409 (2011)

Thermal oscillations of structurally distinct single-walled carbon nanotubes

Polina Pine[*]
Russel Berrie Nanotechnology Institute, Technion, Haifa 32000, Israel

Yuval E. Yaish[†]
Department of Electrical Engineering, Technion, Haifa 32000, Israel

Joan Adler[‡]
Department of Physics, Technion, Haifa 32000, Israel

(Received 5 September 2011; published 9 December 2011)

Zigzag, armchair, and different types of chiral single-walled carbon nanotubes (SWCNTs) have distinct structures, due to different wrapping vectors of the underlying graphene sheets. The electronic properties depend on their structure, but this is less clear with regard to their mechanical properties. We modeled the first four flexural thermal vibrational modes of all three types with clamped ends, as a function of length. We applied a carefully equilibrated molecular dynamics procedure that was previously validated by comparison with the Timoshenko beam model in suitable limits. This analytic model allows for both rotary inertia and shearing deformation, but it cannot differentiate among the three atomistic structures. Comparison between the vibrational behavior of the three types of nanotubes clearly shows that the SWCNT structure does not affect the vibrational frequencies under clamped conditions.

DOI: 10.1103/PhysRevB.84.245409 PACS number(s): 62.25.−g

I. INTRODUCTION

Carbon nanotubes (CNTs) possess unique electrical and mechanical properties and are of great interest for both basic and applied research. One active research field is that of nanoelectromechanical systems (NEMSs) based on CNTs.[1,2] With respect to conventional NEMSs, CNTs are extremely light, have very high Young's moduli ($E \sim 1$–5 TPa), and contain a small number of structural defects. It is anticipated that they will oscillate at high frequencies with high-quality factors, allowing unprecedented mass sensitivity.[3–7] The vibrational frequencies of CNTs are sensitive to the applied external load and the frequency shifts under an external perturbation.

Nanotubes have three main geometrical classifications — armchair, zigzag and chiral — due to the different wrapping vector (n,m) values of the underlying graphene sheets. Experiments and some theories show differences in electronic properties among the different types and subtypes.[8–10] Several older studies[11,12] claim that there is no difference in the mechanical properties of the different classifications, without providing extensive data. One molecular mechanics study[13] clearly shows that for nanotubes that are not doubly clamped, radial breathing modes differ for different structures, and the atomistic study by Huang *et al.*[14] proposes that chirality may be relevant in calculations of Young's modulus.

Many numerical studies of vibrations[15–25] either are based on continuum models or, if atomistic, consider only a single type of tube. In a continuum analytic model it is hard to differentiate among the different atomistic structures. Another force constant study[26] for a large range of different types and sizes of nanotubes found some distinctions among types. Sânchez-Portal *et al.*[27] also found some dependence on nanotube radius in an *ab initio* study. A recent study[28] provides accurate parameters for all types of nanotubes and shows that the simple expression[8] for the radius as a function of n and m is more complex,[29] thereby further emphasizing the need to use atomistic models. We are unaware of a comphrehensive study that considers the effect of structure on multiple lateral modes of doubly clamped SWCNTs, and in view of the above-described contradictions, this issue requires clarification.

In a recent paper[30] we reported carefully equilibrated molecular dynamics (MD) simulations of doubly clamped armchair single-walled carbon NTs (SWCNTs) including a precise analysis of the four lowest modes of vibrations. We provided clear evidence for the failure of simple analytic models such as Euler-Bernoulli (EB) to accurately extract resonance frequencies, as the ratio (R/L) between the tube radius (R) and the length (L) varies. Our results were in excellent agreement with the Timoshenko beam[31] model, which includes the effect of both rotary inertia and of shearing deformation.

Invoking the EB model implies that the bending rigidity (which is the product of E and the nanotube wall thickness) is constant. We showed that if λ_n is the wavelength of the nth mode, for higher values of R/λ_n this is most definitely not true. Yakobson's paradox[32] relates to a scatter of between 1 and 5 TPa in the Young's modulus from atomistic simulations. We shed light on this by giving an upper cutoff estimate for the effective SWCNT thickness and showed that, in the Timoshenko model, there are two sources for the nanotube thickness. The issue of nanotube thickness was also addressed in Ref. 14 from a different viewpoint, and our E and thickness results are in good agreement.

The results in Ref. 11, claiming independence of nanotube type, while impressive for that time, are based on the old inaccurate expression for the nanotube radius, simplified force field potentials, and use the EB expressions to translate among Young's modulus, tube radius, and vibrational frequency. Statements in Ref. 12 are based on Ref. 11 and, hence, are not independent. As explained above, understanding vibrational

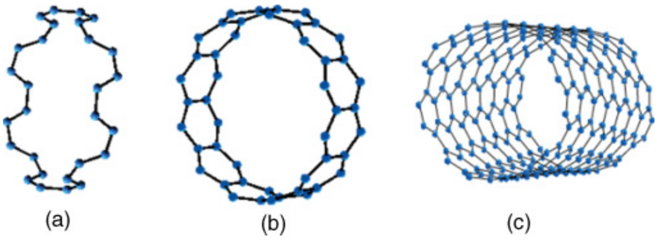

FIG. 1. (Color online) Unit cell of (a) a (7,7) armchair denoted A, (b) a (12,0) zigzag (Z), and (c) an (8,6) chiral nanotube denoted C1. The other chiral type [C2, (9,6)] has an even longer unit cell.

behavior is more subtle than the simple deductions made in Refs. 11 and 12 from the EB model. The results in Ref. 13 showing dependence on nanotube type are consistent with the Timoshenko model and do not invoke old expressions for the radius. However, they are not relevant to the case of doubly clamped lateral modes, thus this case remains open.

II. OUR SIMULATIONS

We report below on the vibrational behavior of four types of SWCNTs: armchair (denoted A), zigzag (Z), and two chiral ones (C1 and C2). We use the approach that we carefully validated for the armchair case in Ref. 30. We generate high-quality data with MD simulations on carefully equilibrated clamped tubes (using the Brenner[33] potential) for the thermal vibrations decomposed into different modes. We obtain the dependence of the four lowest modes on length for each of these four nanotubes. Details about the computational procedure and its validation from the Timoshenko beam model can be found in Ref. 30. Throughout the code development we generated still and animated atomic images with AViz[34,35] for verification purposes.

SWCNTs are periodic and consist of a specific number of repetitive unit cells. The number of unit cells for a given length varies widely between types. For example, a (7,7) armchair nanotube (A) with $L = 66.41$ Å consists of 27 periods with 28 atoms in every unit cell, a (12,0) zigzag nanotube (Z) with $L = 68.16$ Å consists of 16 periods with 48 atoms in each unit cell, an (8,6) chiral nanotube (C1) with $L = 103.65$ Å consists of 4 periods with 296 atoms in every unit cell, and a (9,5) chiral nanotube (C2) with $L = 157.05$ Å consists of only 3 periods with 604 atoms in every unit cell (see Fig. 1 and Tables I and II for more details). In Fig. 1 we show one unit cell for an armchair, a zigzag, and one of the chiral nanotubes. The axis of the nanotube is in the y direction, and we study vibrations in the z direction. (Our validation process included confirming identical (within statistical error) results for vibrations in the x direction for each case). The frequencies of the vibrational modes depend on both L and R; see Ref. 30 for details of the correct dependence for the armchair case.

In order to compare frequencies among different nanotube types, we need to match the radius and length of the different nanotube types as closely as possible. To obtain almost-identical lengths of vibrating segment (L_v) for the four nanotube types, we studied (A, Z, and the two chiral ones, C1 and C2), we clamped (froze) their ends differently for each type. Each vibrating segment was built up from an integer numbers of unit cells, to avoid any possible boundary conditions effects on the vibrational frequencies. The first (last) three periods were frozen for the A's, the first (last) two periods for the Z's, and one first (last) period for the chiral nanotubes. To achieve identical radii we selected suitable chiral vectors that were as close as possible to those of the A and Z tubes. The radii of the nanotubes of types A, Z, C1, and C2 are 4.75, 4.70, 4.76, and 4.81Å, respectively, and details of the total length and of the length of the vibrating segments for all cases are given in Tables I and II.

TABLE I. Data sets of length and vibrating length of our A [zigzag (7,7)] and Z [armchair (12,0)] nanotubes.

(7,7) Zigzag nanotubes			(12,0) Armchair nanotubes		
L (Å)	L_v (Å)	No. of periods	L (Å)	L_v (Å)	No. of periods
66.41	51.65	27	68.16	49.36	16
93.48	78.71	38	93.72	76.68	22
120.52	105.76	49	123.54	106.50	29
147.57	132.81	60	153.36	134.56	36
196.76	182.0	80	204.48	185.68	48
245.95	231.19	100	255.60	236.80	60
295.14	280.38	120	306.72	287.92	72

We used the Brenner potential, which allows for electronic density indirectly in calculating the atomic locations. It has been shown that nanotube distortions can influence their band structure[36–40] in a different way for different chiralities. The distortions investigated were of the order of several nanometers, whereas the movements for our lateral deformations are only about $\sim 10^{-1}$ Å, hence causing insignificant modification of the nanotube's band structure. Two thermodynamic ensembles were tested: canonical and microcanonical. No substantial difference in average frequency values was found and we present the canonical ensemble results below. In order to maintain a constant temperature, a Berendsen thermostat[41] was applied. To ensure stable nanotube structure and eliminate intrinsic tension, we collected data after a period of slow initial thermalization to 300 K (periodic boundary conditions with

TABLE II. Data sets of length and vibrating length for our chiral (8,6) and (9,5) nanotubes (NTs).

L(Å)	L_v(Å)	No. of periods
	(8,6) Chiral NTs	
103.65	51.83	4
129.56	77.74	5
155.48	103.65	6
181.39	129.56	7
207.30	155.48	8
233.21	181.39	9
	(9,5) Chiral NTs	
157.05	52.35	3
209.4	157.05	4
261.75	209.4	5
314.1	261.75	6

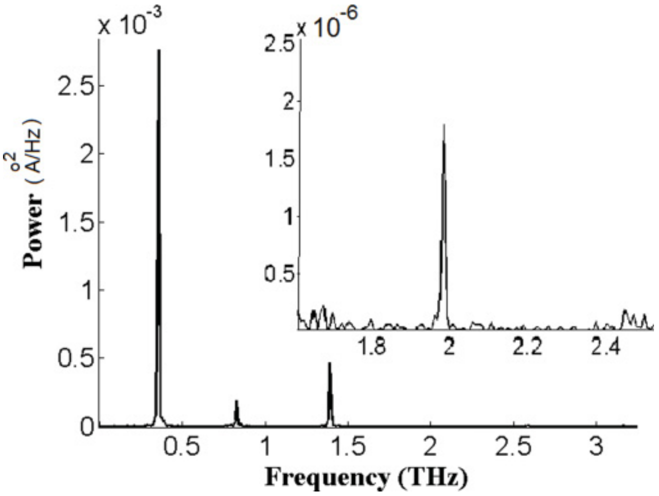

FIG. 2. FFT analysis of the first four thermal vibrational modes (n = 1−4) in the z direction at a point near the center of mass at 300 K for the (8,6) chiral nanotube (C1). The inset is a zoom into the $4th$ vibrational mode.

no frozen edges), waiting until the length of the equilibrated nanotube remained constant up to insignificant fluctuations. Since a large number of SWCNTs with different chiralities and lengths were studied, the number of data needed for the vibrational analysis was reduced by selecting some special points where data were recorded (see Ref. 30 for details). In order to obtain adequate statistics for all vibrational modes we let every nanotube vibrate 1000 times more than the period of its lowest frequency, using an MD time step of 0.5 fs. We then applied a fast Fourier transform (FFT) analysis to the data from the selected points (including one near the center of mass) to calculate the power density as a function of frequency for each of the 24 nanotubes. For example, Fig. 2 depicts vibrational modes after the FFT analysis for the shortest (8,6) chiral nanotube. Its power density versus frequency is presented for the first four thermal vibrational modes ($n = 1$–4) in the z direction at 300 K, and the inset zooms into the fourth vibrational mode, with a much lower oscillation amplitude.

III. RESULTS

In Fig. 3 we show the frequencies of the first four modes as a function of the length of the nanotubes, with the types given in the legend. The graph includes raw data and interpolated lines which are explained below. We observe no substantial differences in vibrational behavior among the three nanotube types or between the two chiral nanotubes. In order to confirm this observation further we studied the changes in relative frequencies ($\frac{\delta f}{f}$). For this purpose, identical lengths of four chiral vector nanotubes are needed at each point. To achieve this we implemented a procedure that interpolates between any two adjacent points with the following length dependence: $f = \frac{a}{L} + \frac{b}{L^2}$ (see solid lines in Fig. 3). Relative frequency changes are calculated using these interpolated data. Figure 4 depicts the frequency changes of A, C1, and C2 nanotubes relative to those of zigzag nanotubes for the first four vibrational modes

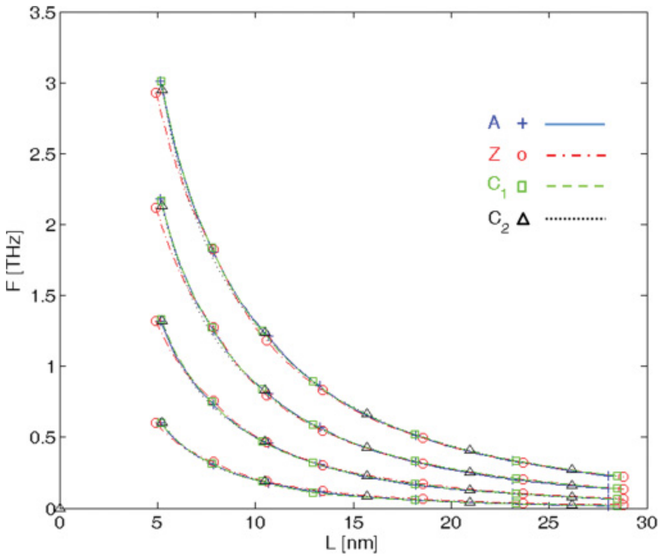

FIG. 3. (Color online) Frequencies of the first four vibrational modes as a function of length. Symbols and lines are defined in the legend, where solid lines represent the interpolation result and symbols represent experimental data.

according to Eq. (1),

$$\frac{\delta f}{f} = \frac{(f - f_{\text{nanotube}})}{f_{\text{nanotube}}}, \tag{1}$$

where f_{nanotube} is the frequency of the nanotube type we compare with (in the case of Fig. 4, f_{nanotube} is f_Z). The inset shows the same changes for the fourth vibrational mode only. Since $\delta f/f$ is close to 0, it can be concluded from Fig. 4 that no substantial difference between the nanotubes could be detected. We carried out the same procedure relative to the frequencies of the A nanotubes. The graphs are qualitatively

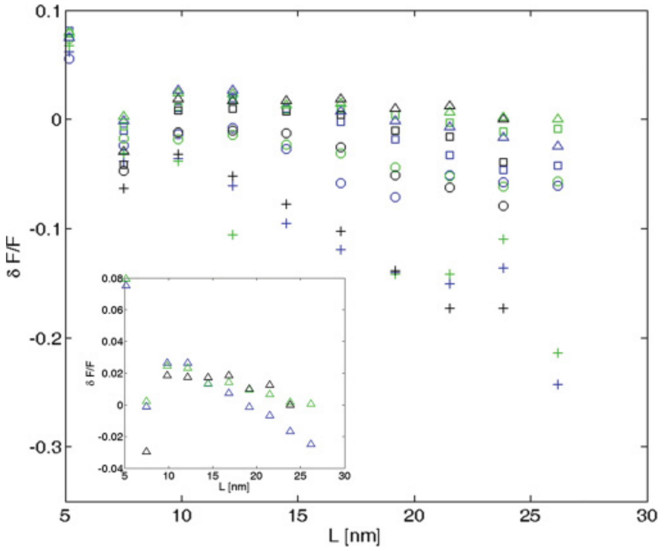

FIG. 4. (Color online) Relative frequency $\frac{\delta f}{f}$ changes relative to the frequencies of the zigzag nanotubes of the first four vibrational modes of the other tubes as a function of L_v. Blue, green, and black refer to the A, C1, and C2 nanotubes, respectively. The symbols $+$, $\circ$, $\square$, and $\triangle$ depict the first, second, third, and fourth modes, respectively. Inset: Relative frequency dependency of the fourth mode only.

similar and no substantial difference among the four nanotube types was detected. These studies provide a systematic set of comparisons between distinct structures and radii within a high-quality classical potential model. We note that our tubes are relatively short and plan to extend the length in future studies. A recent continuum study of longer nanotubes[42] showed that thermal fluctuations may induce strong coupling between resonance modes. This could result in frequency shifts. It is not realistic at this time to attempt such a study with full *ab initio* modeling, and we do not expect that it would affect the trends in the results.

IV. CONCLUSIONS

Our results show that the vibrational behavior of doubly clamped SWCNTs does not depend on the type or chirality (in other words, on the types and subtypes) of the nanotube (armchair, zigzag, or chiral). Moreover, a change of the chiral vector of one of the nanotube types (as long as the radius does not change by more than ±0.5 Å; in our case, 4.76 and 4.81 Å are the radii of the C1 and C2 chiral nanotubes, respectively) does not affect the vibrational frequencies. This is useful for the design of ultrahigh NEMS sensors because it shows that one can select the nanotube without making allowance for the chirality. These results are based on extreme care both with equilibration and with the matching or interpolation of radii and lengths. We have shown that the frequencies of the lateral modes of doubly clamped SWCNTs depend only on the nanotube length and radius, and not on the nanotube type.

ACKNOWLEDGMENTS

We thank the Russell Berrie Nanotechnology Institute for support via the NEVET program, use of the NANCO computer, and a fellowship for P.P. Y.E.Y thanks the ISF (Grant No. 1334/06) for support. P.P. thanks the Ramon Foundation and the Israel Industrial Club for financial support.

---

[*] pine@tx.technion.ac.il
[†] yuvaly@ee.technion.ac.il
[‡] phr76ja@tx.technion.ac.il

[1] R. Ruoff and D. Lorents, Carbon **33**, 925 (1995).

[2] D. Srivastava, M. Menon, and K. Cho, Comput. Sci. Eng. **3**, 42 (2001).

[3] V. Sazonova, Y. Yaish, H. Ustunel, D. Roundy, T. A. Arias, and P. L. McEuen, Nature **431**, 284 (2004).

[4] K. Jensen, K. Kim, and A. Zettl, Nano Lett. **8**, 4342 (2008).

[5] A. K. Huttel, G. A. Steele, B. Witkamp, M. Poot, L. P. Kpuwenhoven, and H. J. van der Zant, Nano Lett. **9**, 2547 (2009).

[6] B. Lassagne, D. Garcia-Sanchez, A. Aguasca, and A. Bachtold, Nano Lett. **8**, 3735 (2008).

[7] H.-Y. Chiu, P. Hung, W. C. Postma, and M. Bockrath, Nature Nanotech. **3**, 533 (2008).

[8] R. Saito, G. Dresselhaus, and M. S. Dresselhaus, *Physical Properties of Carbon Nanotubes*, 1st ed. (World Scientific, Singapore, 1998).

[9] Yu. N. Gartstein, A. A. Zakhidov, and R. H. Baughman, Phys. Rev. B **68**, 115415 (2003).

[10] G. D. Mahan, Phys. Rev. B **68**, 125409 (2003).

[11] J. P. Lu, Phys. Rev. Lett. **79**, 1297 (1997).

[12] H. Ustunel, D. Roundy, and T. A. Arias, Nano Lett. **5**, 523 (2005).

[13] S. S. Gupta, F. G. Bosco, and R. C. Batra, J. Appl. Phys. **106**, 063527 (2009).

[14] Y. Huang, J. Wu, and K. C. Hwang, Phys. Rev. B **74**, 245413 (2006).

[15] A. F. Qvila, G. Silveira, and R. Lacerda, Mater. Res. **11**, 325 (2008).

[16] T. Natsuki, K. Tantrakarn, and M. Endo, *Appl. Phys. A* **79**, 117 (2004).

[17] V. P. Veedu, D. Askari, and M. N. Ghasemi-Nejhad, J. Nanosc. Nanotech. **6**, 2159 (2006).

[18] G. Cao, X. Chen, and J. W. Kysar, Phys. Rev. B **72**, 235404 (2005).

[19] Y. I. Prylutskyy, S. S. Durov, O. V. Ogloblya, E. V. Buzaneva, and P. Scharff, Comput. Mater. Sci. **17**, 352 (2000).

[20] Q. Wang, J. Appl. Phys. **98**, 124301 (2009).

[21] Y. Q. Zhang, G. R. Liu, and X. Y. Xie, Phys. Rev. B **71**, 195404 (2005).

[22] K. Sohlberg, B. Sumpter, R. Tuzun, and D. Noid, Nanotechnology **9**, 30 (1998).

[23] J. Yoon, C. Ru, and A. Mioduchowski, Composite Sci. Technol. **63**, 1533 (2003).

[24] C. Li and T. Chou, Int. J. Solids Struct. **40**, 2487 (2003).

[25] C. To, Finite Elements Anal. Design **42**, 404 (2006).

[26] V. Popov, Mater. Sci. Eng. R **43**, 61 (2004).

[27] D. Sanchez-Portal, E. Artacho, J. M. Soler, A. Rubio, and P. Ordejon, Phys. Rev. B **59**, 12678 (1999).

[28] R. K. F. Lee, B. J. Cox, and J. M. Hill, J. Phys. A **42**, 065204 (2009).

[29] T. Vogel, T. Mutat, J. Adler, and M. Bachmann, Phys. Proc. **15**, 87 (2011)

[30] P. Pine, Y. E. Yaish, and J. Adler, Phys. Rev. B **83**, 155410 (2011).

[31] S. P. Timoshenko and J. N. Goodier, *Theory of Elasticity*, 3rd ed. (McGraw–Hill, New York, 1987).

[32] O. A. Shenderova, V. V. Zhirnov, and D. W. Brenner, Crit. Rev. Solid State Mater. Sci. **27**, 227 (2002).

[33] D. W. Brenner, Phys. Rev. B **42**, 9458 (1990).

[34] J. Adler, A. Hashibon, N. Schreiber, A. Sorkin, S. Sorkin, and G. Wagner, Comput. Phys. Commun. **147**, 665 (2002).

[35] J. Adler and P. Pine, Comput. Phys. Commun. **180**, 580 (2009).

[36] R. Heyd, A. Charlier, and E. McRae, Phys. Rev. B **55**, 6820 (1997).

[37] L. Yang, M. P. Anantram, J. Han, and J. P. Lu, Phys. Rev. B **60**, 13874 (1999).

[38] L. Yang and J. Han, Phys. Rev. Lett. **85**, 154 (2000).

[39] E. D. Minot, Y. Yaish, V. Sazonova, J. Y. Park, M. Brink, and P. L. McEuen, Phys. Rev. Lett. **90**, 156401 (2003).

[40] J. Cao, Q. Wang, and H. Dai, Phys. Rev. Lett. **90**, 157601 (2003).

[41] H. Berendsen, J. Postma, W. van Gunsteren, A. DiNola, and J. Haak, J. Chem. Phys. **81**, 3684 (1984).

[42] A. W. Barnard, V. Sazonova, A. M. van der Zande, and P. L. McEuen, e-print arXiv:1110.1517 [cond-mat].